DP-MS-82-32 Rev. 1

EXPERIMENTAL SUPPORT FOR A PREDICTIVE OSMOTIC MODEL OF CLAY MEMBRANES

by

Steven J. Fritz

Department of Geology
Texas A&M University
College Station, Texas 77843

and

I. Wendell Marine

E. I. du Pont de Nemours & Co.
Savannah River Laboratory
Aiken, South Carolina 29808

For publication
Geochimica et Cosmochimica Acta

This paper was prepared in connection with work done under Contract No. DE-AC09-76SR00001 with the U.S. Department of Energy.

This document was prepared in conjunction with work accomplished under Contract No. DE-AC09-76SR00001 with the U.S. Department of Energy.

DISCLAIMER

EXPERIMENTAL SUPPORT FOR A PREDICTIVE OSMOTIC MODEL OF CLAY MEMBRANES *

by

Steven J. Fritz
Department of Geology
Texas A&M University
College Station, Texas 77843

and

I. Wendell Marine

E. I. du Pont de Nemours & Co.
Savannah River Laboratory
Aiken, South Carolina 29801

ABSTRACT

Osmosis has been cited as a mechanism for explaining anomalously high fluid pressures in the subsurface. Clays and shales act as membranes, and osmotic flux across these units may result in pressures sufficiently high to explain these anomalies. The theoretical osmotic pressures as calculated solely from solution properties can be quite large; however, it is not yet resolved whether these geologic membranes are sufficiently ideal to generate such pressures.

Osmotic efficiencies of a Na-bentonite membrane were measured by a series of hyperfiltration experiments using various molarities of NaCl at two different porosities. The highest osmotic efficiency (0.8912) occurred at the lower porosity and the lowest NaCl input solution. The lowest measured osmotic efficiency (0.0423) occurred at the higher porosity and the highest NaCl input concentration.

*The information contained in this article was developed during the course of work under Contract No. DE-AC09-76SR00001 with the U.S. Department of Energy.

The osmotic efficiencies obtained from the hyperfiltration experiments correlate very favorably with the Fritz-Marine Membrane Model. This model predicts that the maximum osmotically-induced hydraulic pressures in the subsurface should occur across shales having low porosities and high cation exchange capacities in which the unit separates solutions of brackish waters.

INTRODUCTION

That clays and shales act as membranes is well documented by experiment. Clay membranes have been found to generate electro-osmotic effects (Hanshaw, 1963; Srivastava and Avasthi, 1975), hyper-filtration of both solutes and stable isotopes (Kharaka and Berry, 1973; McKelvey and Milne, 1962; Coplen and Hanshaw, 1973) as well as osmotic effects (Young and Low, 1965; Kemper and Rollins, 1966; Olsen, 1969).

Because clays and shales act as membranes, they are capable of generating osmotic pressures in the subsurface. If these units separate solutions of different aqueous activities, the resultant osmotic flux is capable of generating fluid pressures of hundreds of bars. Marine and Fritz (1981) reported that two wells penetrating a basin in South Carolina containing saline water had hydrostatic heads 82 and 134 meters above the pieziometric surface of the fresh-water aquifer above. The theoretical osmotic pressure calculated from the chemical composition of the water from these well samples agreed within 5 percent of the actual heads. Hanshaw and Hill (1969) and Bredehoeft et al. (1963) have also reported evidence supporting osmotically-generated hydrostatic pressures. Hanshaw and Zen (1965) suggest that osmotic pressure across shale beds may be important in facilitating thrust faults. In the siting of a subsurface waste repository where shale beds are nearby, an understanding of the osmotic effects on hydraulic heads is essential for a complete understanding of the subsurface hydrology. The possibility of osmotically-induced fracturing of shale aquitards has been discussed by Hanshaw (1972).

Since clays are non-ideal membranes, the maximum osmotic pressure generated across theses units is less than that predicted for ideal membranes. Yet to be resolved is whether these geologic membranes are sufficiently ideal to generate anomalously high fluid pressures in the subsurface. The ideality of a clay membrane is a function of the membrane's cation exchange capacity and porosity as well as the concentration of solutes in which the membrane is imbibed (Marine and Fritz, 1981). Osmotic efficiency is greatest when a low porosity clay membrane having a high cation exchange capacity separates dilute solutions. Marine and Fritz (1981) derived a mathematical model relating osmotic efficiency of clay membranes to these parameters, and they showed that clay membranes approach ideal behavior as the porosity tends toward zero.

The intent of this investigation is to test by experiment the osmotic efficiency model of Marine and Fritz (1981) and to use the experimental data to support or deny the contention that osmosis is a viable mechanism for producing anomalously high fluid pressures in the subsurface. The osmotic efficiency data were obtained by a hyperfiltration method in which different concentrations of NaCl were hydraulically forced through a Na-bentonite membrane at two different porosities and a constant hydraulic pressure gradient.

SYMBOLS AND UNITS

The following is a list of all symbols used in derivations and calculations. Dimensionality of the SI units are enclosed in brackets.

C concentration of solute in moles$\cdot$cm^{-3} [M L^{-3}]

C_a concentration of a univalent anion in free solution in moles$\cdot$cm^{-3} [M L^{-3}]

$\overline{C}_a$ concentration of a univalent anion within the Donnan Double Layer in moles·cm^{-3} [M L^{-3}]

$\overline{C}_c$ concentration of a univalent cation within the Donnan Double Layer in moles·cm^{-3} [M L^{-3}]

C_e steady state concentration of solute exiting membrane at the low pressure side of membrane in moles·cm^{-3} [M L^{-3}]

C_i solute concentration in reservoir unaffected by concentration polarization in moles·cm^{-3} [M L^{-3}]

C_o steady state concentration of solute entering the high pressure side of the membrane in moles·cm^{-3} [M L^{-3}]

C_x solute concentration at any point, x, within the concentration polarization layer in moles·cm^{-3} [M L^{-3}]

$\overline{C}_x$ solute concentration per unit area of porous frit surface in moles·cm^{-2} [M L^{-2}]

D unidirectional diffusion coefficient of solute in cm^2·sec^{-1} [L^2 t^{-1}]

E cation exchange capacity of membrane in equivalents·gram^{-1} [Dimensionless]

f_{aw} frictional coefficient between a mole of anion in the membrane and an infinite amount of water in the membrane in dyne·sec·mole^{-1}·cm^{-1} [t^{-1}]

f_{cw} frictional coefficient between a mole of cations in the membrane and an infinite amount of water in the membrane in dyne·sec·mole^{-1}·cm^{-1} [t^{-1}]

f_{am} frictional coefficient between a mole of anions in the membrane and an infinite amount of solid membrane matrix in dyne·sec·mole^{-1}·cm^{-1} [t^{-1}]

f_{cm} frictional coefficient between a mole of cations in the membrane and

an infinite amount of solid membrane matrix in dyne·sec·mole^{-1}·cm^{-1} [t^{-1}]

J_d flux of salt diffusing away from the high pressure side of the membrane in moles·cm^{-2}·sec^{-1} [M L^{-2} t^{-1}]

J_m salt flux through the membrane in moles·cm^{-2}·sec^{-1} [M L^{-2} t^{-1}]

J_s flux of salt directed unidirectionally toward high pressure membrane face by hydraulic force in moles·cm^{-2}·sec^{-1} [M L^{-2} t^{-1}]

J_v flux of solution directed unidirectionally toward high pressure membrane face by hydraulic force in moles·cm^{-2}·sec^{-1} [M L^{-2} t^{-1}]

C_s arithmatic mean of solute concentration across the membrane in moles·cm^{-3} [M L^{-3}]

K the filtration coefficient [Dimensionless]

K_s distribution coefficient of the solute within the pores of the membrane [Dimensionless]

L_p solution permeability coefficient in cm^3·dyne^{-1}·sec^{-1} [L^2 t M^{-1}]

R_m a ratio of frictional coefficients (= f_{cm}/f_{am}) [Dimensionless]

R_w a ratio of frictional coefficients (= f_{cw}/f_{aw}) [Dimensionless]

R_{wm} a ratio of frictional coefficients (= f_{am}/f_{aw}) [Dimensionless]

t_c° cation transport number in free solution [Dimensionless]

x_i the position in the high pressure reservoir marking the onset of hyperfiltration, in cm [L]

ΔP hydraulic pressure across membrane in dyne·cm^{-2} [M L^{-1} t^{-2}]

$\Delta\Pi$ osmotic pressure across the membrane in dyne·cm^{-2} [M L^{-1} t^{-2}]

ρ dry density of minerals comprising membrane in gram·cm^{-3} [M L^{-3}]

σ the reflection coefficient [Dimensionless]

ϕ_w porosity of the membrane [Dimensionless]

χ concentration of fixed negative charges of the solid membrane

matrix in moles·cm^{-3} [M L^{-3}]

ω solute permeability coefficient in moles·dyne^{-1}·sec^{-1} [t L^{-1}]

THEORETICAL CONSIDERATIONS

Hyperfiltration, or "reverse osmosis," is a process by which solution is hydraulically forced through a membrane causing a build-up of solute on the high pressure (upstream) side of the membrane and a dilution of solute on the low pressure (downstream) side. On the high pressure side of the membrane, the solute concentration is greatest at the membrane/solution interface (Figure 1). The solute concentration decreases away from this interface out into the high pressure fluid reservoir until, at some distance away from the interface, the solute concentration equals that of the reservoir. The distance between this point and the high pressure interface is the "concentration polarization layer," or CPL (Porter, 1979). Under steady state conditions, the profile of the CPL is constant.

Figure 1 is a diagram of hyperfiltration through a clay membrane positioned between two sandstone units. (These hypothetical lithologies are analagous to the two porous frits bounding the clay membrane in the hyperfiltration experiments). The following derivation holds for unidirectional flux in the direction perpendicular to the membrane face with fluxes measured positively from left-to-right.

The salt flux through the membrane is given by the continuity equation:

$$\frac{\partial C}{\partial t} = - \text{Div } J_m = - \frac{\partial J_m}{\partial x} \qquad (1)$$

The salt exiting the membrane at x_e is the difference of salt advected toward the membrane by hydraulic forces (J_s) and the salt diffusing away from the high pressure interface (J_d).

$$J_m = J_s - J_d \tag{2}$$

These fluxes have units of moles$\cdot$cm$^{-2}\cdot$sec^{-1}. The salt advected towards the membrane is simply equal to the solution flux (J_v in cm$\cdot$sec^{-1}) times its concentration (C in moles$\cdot$cm^{-3}).

$$J_s = C \cdot J_v \tag{3}$$

The unidirectional back diffusion of salt away from the high pressure interface can be expressed by Fick's Law:

$$J_d = -D \frac{\partial C}{\partial x} \tag{4}$$

where D is the diffusion coefficient of the solute in the x direction. Combining (2) and (4) and substituting into (1) yields

$$\frac{\partial C}{\partial t} = -J_v \frac{\partial C}{\partial x} - D \frac{\partial^2 C}{\partial x^2} \tag{5}$$

At steady state $\partial C/\partial t = 0$, such that

$$\frac{d^2C}{dx^2} = \frac{-J_v}{D} \cdot \frac{dC}{dx} \tag{6}$$

Upon integration,

$$\frac{dC}{dx} = A \cdot \exp(-J_v \cdot x/D), \tag{7}$$

where A is a constant of integration.

At steady state it is assumed that the ratio of concentration of salt exiting the membrane at x_e (C_e) to that entering the membrane at x_o (C_o) is a constant, K, such that

$$K = \frac{C_e}{C_o} \tag{8}$$

This constant, K, is hereby defined as the filtration coefficient,

and its value ranges from zero for ideal membranes to unity for porous media having no membrane properties.

Thus, the steady state flux of salt exiting the membrane at x_e is equal to the salt concentration at that interface times the steady state advective solution flux, J_v.

$$J_m = C_e \cdot J_v = C_o K \cdot J_v \tag{9}$$

At steady state the salt flux at the high pressure interface (x_o) is

$$J_m = J_s - J_d = C_o \cdot J_v + D \frac{dC}{dx} \tag{10}$$

Solving for dC/dx in (10) and evaluating this differential at x=0 yields

$$(dC/dx)_{x=0} = - \frac{C_o (1-K) \cdot J_v}{D} \tag{11}$$

At x=0, dC/dx also equals the integration constant ,A, in (7) such that

$$(dC/dx)_{x=0} = A \cdot \exp(-J_v \cdot x/D) = A = - \frac{C_o (1-K) \cdot J_v}{D} \tag{12}$$

Substitutimg this value of A into (7) obtains

$$\frac{dC}{dx} = - \frac{C_o (1-K) \cdot J_v}{D} \cdot \exp(-J_v \cdot x/D) \tag{13}$$

This is the slope of the profile of the concentration polarization layer at any distance x away from the high pressure interface. If the membrane is non-permselective, then K=1 and $C_i = C_o = C_e$. In this case, the concentration profile in Figure 1 would be a straight line perpendicular to the membrane face and the slope of that line would be zero. This can be verified by substituting a value of unity for K in equation 13.

Upon integration of (13)

$$C_x = C_o (1-K) \cdot \exp(-J_v \cdot x/D) + Q \tag{14}$$

where C_x is the salt concentration at any point x within the CPL and

Q is a constant of integration.

To evaluate Q we employ the boundary condition that, at x_i, the concentration of solution is unaffected by the CPL (Fig. 1), and hence is equal to the concentration of salt in the reservoir, C_i. Thus

$$C_i = C_o(1-K) \cdot \exp(-J_v \cdot x_i/D) + Q \tag{15}$$

Solving for Q obtains

$$Q = C_i - C_o(1-K) \cdot \exp(-J_v \cdot x_i/D) \tag{16}$$

Substituting (16) into (14) and arranging terms yields

$$C_x = C_o(1-K) \cdot [\exp(-J_v \cdot x/D) - \exp(-J_v \cdot x_i/D)] + C_i \tag{17}$$

At the high pressure interface, x=0 and $C_x=C_o$ such that

$$C_o = \frac{C_i}{K + (1-K) \cdot \exp[-J_v \cdot x_i/D]} \tag{18}$$

Equation 18 relates the solute concentration at the high pressure interface of the membrane (C_o) to the initial concentration in the reservoir system (C_i), the steady state solution flux (J_v), and the diffusion coefficient of the salt (D). The outer limit of the CPL is defined by x_i such at x_i equals the thickness of the CPL (x_i-x_o). For ideal membranes, no salt exits the membrane; hence, $C_e=0$ and $K = C_e/C_o = 0$. In this case $C_o = C_i \cdot \exp(+J_v \cdot x_i/D)$. If the porous medium has no membrane properties, then K=1 and $C_i=C_o=C_e$.

EXPERIMENTAL PROCEDURES

Fifty six grams of dry bentonite (ρ = 2.4 grams$\cdot$cm^{-3}) were mixed with distilled water to make a slurry. This slurry was de-aerated and compacted between two pistons by a manually operated hydraulic jack (Figure 2). The cation exchange capacity of the bentonite was measured to be 98 meq/100 grams. The surface area of the membrane is a constant

81.07 cm^2. In runs 1, 2, and 3 the thickness of the membrane was gauged by a micrometer measurement to be 0.7 cm. This translates to a membrane porosity of 59 percent. The average hydraulic conductivity in these runs is 1.5×10^{-11} $cm \cdot sec^{-1}$. Each run was characterized by hyperfiltrating different molarities of NaCl stock solution through the membrane at a constant ΔP of 17.5 MPa. In runs 4, 5, and 6, the same bentonite was further compacted to yield a porosity of 41 percent, and the same sequence of NaCl solutions was hyperfiltrated (Table 1). The average hydraulic conductivity in these runs is 7.3×10^{-12} $cm \cdot sec^{-1}$. All experimental runs were performed at a constant room temperature of 23° C.

Figure 2 shows the hyperfiltration set-up. A precision, high pressure syringe pump pushes the NaCl solution through the axial port of the top piston. The solution travels sequentially through a 1.27 cm-thick porous frit, the clay membrane, the porous frit of the bottom piston and into the axial port of the bottom piston. The purpose of the frits is to facilitate linear flow paths through the clay membrane. The solution exits into a pre-weighed, stoppered 250 ml Erlenmeyer flask.

Periodically, the needle valve on the high pressure side of the system is opened to tap the solution. When this valve is opened, some solution is bypassed at the frit/piston interface through an annular port in the top piston. It is assumed that the tapped solution is drawn solely from the reservoir in the axial port of the top piston such that the CPL layer within the frit is not perturbed. This tapped solution, representing the solution at the frit/piston interface, is analyzed to insure that the concentration at this interface is kept equal to the concentration in the pump reservoir. This periodic flushing insures no build-up of solute concentration at the piston/frit interface by the concen-

tration polarization effect. Hence, the frit thickness is equal to the CPL with C_o being the concentration at the clay/frit interface and C_i being the concentration at the piston/frit interface.

The evaluation of C_o by equation 18 requires a knowledge of the filtration coefficient, K. This can be determined by a mass balance calculation. If the total amount of salt present in the porous frit at steady state is known, then it is possible to calculate the value of K, and ultimately C_o. This is possible because the build-up of solute due to the concentration polarization effect resides solely in the frit of a known porous volume (48.6 cm^3).

Equation 17 depicts the salt concentration at any distance x within the CPL. If this equation is integrated with respect to x between the limits of x_o and x_i, then the product of that integration represents the salt concentration per square centimeter of porous frit surface, such that $\overline{C}_x = \int_{x_0}^{x_i} C_x \, dx$. From this definition and equation 17 the integration results in

$$\overline{C}_x = C_o(1-K)\left[\frac{D}{J_v} \cdot \left(1-\exp\left(-\frac{J_v \cdot x_i}{D}\right)\right)-x_i \exp\left(-\frac{J_v \cdot x_i}{D}\right)\right] + C_i x_i \quad (19)$$

Substituting C_e/K for C_o and collecting terms yields

$$\frac{1}{K} = 1 + \frac{1}{C_e}\left[\frac{\overline{C}_x - C_i \cdot x_i}{D/J_v[1 - \exp(-J_v \cdot x_i/D)] - x_i \cdot \exp(-J_v \cdot x_i/D)}\right] \quad (20)$$

During a run, the throughput solution is collected, weighed and analyzed for chloride by silver nitrate titration in the presence of a $Ag/S^=$ electrode. The analytical precision of this method is $\pm$ 0.003 moles Cl^-/cm^3. Since NaCl is the only electrolyte in the solution, the molarity of Cl^- is assumed to be equal to that of Na^+. When the chloride concentration in the throughput solution reached a steady

state value, the run was terminated. At this juncture, the steady state value of J_v is recorded and the steady state effluent solution concentration is C_e. The value of C_i is equal to that at the frit/piston interface which, due to periodic flushing, is equal to the concentration in the high pressure syringe pump. The thickness of the CPL ($x_i - x_o = x_i$) is equivalent to the frit thickness of 1.27 cm.

After terminating a run, the NaCl solution of the pump and the tubing is flushed with and replaced by distilled water. Flushing was deemed complete when the flushed solution showed no detectable chloride content. A pre-weighed flask was fitted to the needle valve on the top piston and the top frit was flushed with water until all the salt had been collected. The volume of the conduits in the top piston's interior was known from pre-run calibrations such that this salt was subtracted from the total millimoles of NaCl collected to obtain the millimoles of NaCl residing in the 48.6 cm^3 frit at steady state. This molarity is multiplied by the frit thickness to obtain $\overline{C}_x$. Using an average value for D_{NaCl} of 1.5 X 10^{-5} $cm^2 \cdot sec^{-1}$ (Harned and Owen, 1958), the steady state filtration coefficient is calculated by means of equation 20.

RESULTS AND DISCUSSION

Data from the six experimental runs are presented in Table 1. These data clearly show how solution concentration and membrane porosity affect the filtration coefficient, K. In runs 1, 2, and 3 the bentonite membrane's porosity is a constant 59 percent but the molarity of the hyperfiltrated NaCl stock solution varies by increments of an order of magnitude. The filtration coefficient increases with in-

creasing concentration input; that is to say, the filtration efficiency decreases with increasing concentration. The same trend occurs in runs 4, 5, and 6. The calculated value of the NaCl concentration at the high pressure interface (C_o) for run 1 is 0.1502 moles$\cdot$cm^{-3}--a value that is fifteen times greater than that on the downstream side of the membrane face (C_e = 0.0103 moles$\cdot$cm^{-3}).

Decreasing the porosity by compaction promotes a greater degree of overlap of the Donnan double layers on the clay micelles. Hence, it should be expected that the filtration efficiency of a clay membrane will increase with decreasing porosity. Runs 4, 5, and 6 represent hyperfiltrations performed on the same bentonite membrane compacted to a new porosity of 41 percent. The same sequence of NaCl input concentrations were performed in runs 4, 5, and 6 as were conducted in runs 1, 2, and 3. Hence, similar concentrations of NaCl input were used in runs 1 and 4, 2 and 5, and 3 and 6.

A decreased porosity does indeed result in an increased filtration efficiency for similar input concentrations. The improvement of filtration efficiency is especially marked in the high concentration runs as evidenced by K = 0.9189 for Run 3 as compared with a value of K equal to 0.5354 for Run 6 (Table 1). In contrast, only a marginal improvement in filtration efficiency is obtained for the runs having a NaCl input concentration of 0.01 M. (Runs 1 and 4). Yet, the concentration polarization effect in these runs is remarkably high as seen by the high C_o/C_i ratios.

Osmotic Efficiency of Clay Membranes

Using the framework of non-equilibrium thermodynamics, Kedem and Katchalsky (1963) derived a series of expressions for transport of ions

and solution through membranes. For an isothermal, isoelectric system, the unidirectional flux of solution (J_v) and solute (J_s) perpendicularly through a membrane is given by:

$$J_v = L_p \cdot \Delta P - \sigma L_p \cdot \Delta \Pi \tag{21}$$

$$J_s = C_s(1-\sigma) \cdot J_v + \omega \cdot \Delta \Pi \tag{22}$$

where ΔP is the hydraulic pressure difference across the membrane and $\Delta \Pi$ is the theoretical osmotic pressure capable of being generated across the membrane as calculated solely from solution properties. Both terms have units of dyne$\cdot$cm^{-2}. The C_s term is the arithmatic mean of solute concentration across the membrane in moles$\cdot$cm^{-3}. The L_p, σ and ω terms are practical phenomenological coefficients. L_p is a permeability coefficient and has units of cm$^3\cdot$dyne$^{-1}\cdot$sec^{-1}. The solute permeability coefficient, ω, (in moles$\cdot$dyne$^{-1}\cdot$sec^{-1}) is a diffusion coefficient of the solute across the membrane. For ideal membranes, $\omega = 0$. Experimentally determined values of ω range from 10^{-13} to 10^{-19} moles$\cdot$dyne$^{-1}\cdot$sec^{-1} in biological membranes (Dainty and Ginzburg, 1964; Goldstein and Solomon, 1960) to 10^{-14} to 10^{-16} moles$\cdot$dyne$^{-1}\cdot$sec^{-1} in synthetic membranes (Katchalsky and Curran, 1965). Elrick et al. (1976) measured ω for a Na-benonite slurry of 90 percent porosity at 3 X 10^{-15} moles$\cdot$dyne$^{-1}\cdot$sec^{-1}. The value of ω in lower porosity clay membranes should be much lower because diffusion through membranes is slowed as the tortuosity increases (Caplan and Mikulecky, 1966).

The reflection coefficient is defined by Staverman (1952) as the ratio of the observed osmotically-induced hydraulic pressure (ΔP) to that calculated solely from solution properties ($\Delta \Pi$). The measurement of σ is performed when $J_v = 0$. Thus

$$\sigma = (\Delta P / \Delta \Pi)_{J_v=0} \tag{23}$$

For ideal membranes, $\sigma = 1$. In this case, the solution flux is totally comprised of the water flux multiplied by its partial molar volume: $J_v = J_w \cdot \overline{V}_w$. If the membrane is ideal, then J_s in equation 22 is zero because solute can be transported neither by advective means ($\sigma = 1$) nor by diffusion ($\omega = 0$). If the porous medium has no membrane properties, that is, non-permselective, then $\sigma = 0$. The phrase "osmotic efficiency" is hereby defined as the reflection coefficient expressed as a percentage. Thus ideal membranes have osmotic efficiencies of 100 percent and non-permselective membranes are zero percent ideal.

Of the three practical phenomenological coefficients, the reflection coefficient, σ, is by far the most informative because its value predicts the expected osmotically-induced hydraulic pressure ($\sigma\Delta\Pi$) in a geological membrane system. Although the reflection coefficient should be measured in a static flux system (i.e., $J_v = 0$), it is possible to measure σ in a hyperfiltration system that has achieved steady state. This is possible because ω in a compacted clay membrane is very small such that the $\omega\Delta\Pi$ term in equation 22 is negligible. Therefore, $J_s \simeq C_s(1-\sigma)\cdot J_v$. Since $C_s = (C_o + C_e)/2$ and $J_s = C_o K \cdot J_v = C_e \cdot J_v$, then

$$\sigma = \frac{C_o - C_e}{C_o + C_e} \qquad (24)$$

Equation 24 can be tested for the consistency of the relationship between σ and K. For ideal membranes, $C_e = 0$ and $\sigma = 1$. For non-permselective membranes, $C_e = C_o$ and thus $\sigma = 0$.

Table 1 shows the values of σ obtained from hyperfiltration data. For runs at a constant porosity, the more dilute the input concentration, the greater the value of σ. Moreover, for runs at the same concentration, higher values of σ occur in lower porosity membranes.

For each run, the theoretical osmotic pressure was calculated from the C_o and C_e values at steady state according to $\Delta\Pi = \nu RT\Delta C$, where $\nu = 2$ for a 1:1 salt like NaCl and $\Delta C = C_o - C_e$. Along with these values in Table 1 are the calculated osmotically-induced back pressure in terms of $\sigma\Delta\Pi$. Note that the highest osmotically-induced hydraulic pressure ($\Delta P = \sigma\Delta\Pi$) occur in membrane systems separating solutions of moderate concentration. If a membrane is imbibed in solutions of low concentration, σ is maximized, but the theoretical $\Delta\Pi$ is low. Alternately, in membrane systems in contact with high salinity, the theoretical $\Delta\Pi$ is very high but the osmotic efficiency may be so low that the system generates little osmotically-induced hydraulic pressure.

This steady state osmotically-induced back pressure affects the steady state solution flux, J_v. In Table 1, the numerical ranking of $\sigma\Delta\Pi$ values at 59 percent porosity is in reverse order of the ranking of J_v. With the exception of Run 6, this trend is maintained in the three runs conducted at 41 percent porosity. These observations can be explained by the fact that the syringe pump delivers solution to the membrane at a constant upstream pressure of 17.5 MPa. If the hydraulic pressure is fixed, then the solution flux varies. The higher the back pressure due to osmotic flux from the low to high pressure side of the membrane, the lower the flux of solution from the high to low pressure side.

CORRELATION OF RESULTS WITH THE FRITZ-MARINE MEMBRANE MODEL

Marine and Fritz (1981) presented a theoretical model predicting the osmotic efficiency of clay membranes based upon the premise that,

under steady state conditions, the thermodynamic forces acting across the membrane are counterbalanced by the sum of mechanical frictional forces acting upon the solution components within the membrane. The end result of that derivation is an equation relating σ to membrane porosity, cation exchange capacity of the membrane matrix and the concentration of solutes in which the membrane is imbibed.

$$\sigma = 1 - \frac{(R_w + 1)K_s}{\{[R_w(\bar{C}_a/\bar{C}_c) + 1] + R_{wm}[R_m(\bar{C}_a/\bar{C}_c) + 1]\}\phi_w} \qquad (25)$$

where $R_w = f_{cw}/f_{aw}$ $\quad R_m = f_{cm}/f_{am}$ $\quad R_{wm} = f_{am}/f_{aw}$

and $K_s = \bar{C}_a/C_a$

and ϕ_w is the water content of the membrane, equal to membrane porosity. R_w represents the ratio of frictional coefficients between the cation and water in the membrane (f_{cw}) to the frictional coefficient between the anion and the water in the membrane (f_{aw}). Likewise, R_m is the ratio of frictional coefficients of the cation and the solid membrane matrix (f_{cm}) to that of the anion and the solid membrane matrix (f_{am}). R_{wm} relates the friction between the anion and the membrane (f_{am}) to that between the anion and the water within the membrane pores (f_{aw}). All frictional coefficients have finite positive values.

K_s is the distribution coefficient of the solute in the membrane and it is expressed as the ratio of the concentration of the anion in the membrane ($\bar{C}_a$) to the concentration of the anion in the outer, or "free solution." Because the net charge of clay surfaces is negative, electroneutrality conditions dictate that the concentration of cations in the charged solution layer adjacent to the net negatively charged clay

micelles be equal to the sum of the anion concentration within this layer plus the concentration of fixed negative charges on the surface of the solid membrane matrix, χ. Thus,

$$\bar{C}_c = \bar{C}_a + \chi \tag{26}$$

For ideal membranes, $\bar{C}_a$ is zero and $K_s = 0$.

The calculation of K_s for a membrane system at equilibrium is obtained by a knowledge of the membrane's porosity (ϕ_w), dry density of the mineral(s) comprising the membrane (ρ in grams$\cdot$cm^{-3}) and cation exchange capacity of the mineral(s) in the membrane (E in equiv$\cdot$gram^{-1}). Thus the concentration of fixed negative exchange sites per unit volume of the clay membrane (χ) can be calculated by:

$$\chi = E\cdot\rho(1-\phi_w) \tag{27}$$

The concentration of the anions per unit volume of the membrane is calculated by

$$\bar{C}_a = -\tfrac{1}{2}\chi + \tfrac{1}{2}(\chi^2 + 4C_s^2\phi_w^2)^{\frac{1}{2}} \tag{28}$$

Equation 28 results from the development of the Teorell-Meyer-Siever membrane model for a univalent salt as expressed by Hanshaw (1962) In this equation all activity coefficients are assumed to be unity.

The frictional resistance between the cation and water in free solution is related to the transport number of the cation in free solution, t_c°, according to Glasstone (1946):

$$\frac{1}{t_c^\circ} = \frac{f_{cw}^\circ + f_{aw}^\circ}{f_{aw}^\circ} = \frac{f_{cw}^\circ}{f_{aw}^\circ} + 1 \tag{29}$$

If the frictional resistance between the cation and anion in the membrane is equivalent to that in the free solution, then

$$\frac{1}{t_c^\circ} = \frac{f_{cw}}{f_{aw}} + 1 = R_w + 1 \tag{30}$$

For NaCl, $t^{\circ}_{Na^+}$ is 0.38 and its value varies less than 10 percent throughout the concentration range of 0 to 3 M NaCl (Miller, 1966). Thus the value of R_w used in equation 25 is 1.63.

R_m relates the relative tendencies of the charged species to be retarded by frictional resistance with the solid membrane structure. If the frictional resistance of the ions is purely physical and hence independent of electrostatic effects, then the ratio of the hydrated radii of cation to anion should give a close approximation of R_m. For NaCl, this ratio is 1.8 (Harned and Owen, 1958).

R_{wm} relates the relative ease of passage of the anion through the membrane in response to an applied physio-chemical gradient. For a highly porous membrane, $f_{aw} >> f_{am}$, and R_{wm} tends toward zero. For a tight membrane, the frictional resistance of the anion with the membrane structure can be quite large such that $f_{aw} << f_{am}$.

Table 2 shows the reflection coefficient calculated from equation 25 along with the salient terms used in that expression. A computer program was written to solve equation 25 with the known parameters using various test values of R_{wm} in increments of 0.01. The "best fit" R_{wm} values in Table 2 are the values of R_{wm} that gave the closest fit of σ calculated by equation 25 with the values of σ obtained by hyperfiltration.

In runs 1, 2, and 3 the porosity is 59 percent. This loose membrane has a framework that is sufficiently open such that the frictional resistance between the anion and water in the membrane greatly exceeds the frictional resistance between the anion and the membrane structure; that is, $f_{aw} >> f_{am}$. This explains why $R_{wm} = 0$ gave the best fit for σ in these runs. When the same bentonite membrane was compacted to 41 percent porosity, the condensed membrane network results in increased frictional

forces between the mobile anion in the membrane and the clay micelles comprising the solid structure. For this reason R_{wm} increases, albeit to a rather small value of 0.10.

Table 2 shows the reflection coefficients as calculated by the Fritz-Marine Membrane Model and that obtained by hyperfiltration. The close agreement between prediction and reality for the reflection coefficient tends to support the validity of this model. This model predicts that osmotic efficiency of clay membranes increases with decreasing porosity and decreasing concentration in which the membrane is imbibed. Moreover, osmotic efficiency should be greatest in membranes having large cation exchange capacities.

CONCLUSIONS

It is possible to determine experimentally osmotic efficiencies of clay membranes by hyperfiltration provided that the determination of solution flux and effluent concentration are measured at steady state.

The theoretical maximum osmotically-induced hydraulic pressure that can be generated across a clay or shale unit can be calculated solely from solution properties on either side of the membrane. However, if the osmotic efficiency of that unit is close to zero then the realized osmotically-induced hydraulic pressure ($\sigma\Delta\Pi$) may be too small to account for anomalously high fluid pressures in the subsurface. In this study it has been shown that osmotic efficiencies of bentonite can be quite high such that the realized osmotically-induced hydraulic pressure in the subsurface can be substantial.

The maximum osmotically-induced hydraulic pressure that could be realized in the subsurface should occur when a low porosity, high cation

exchange capacity shale or clay unit separates solutions of moderate concentration. If the concentration gradient across the clay membrane is very high, then $\Delta\Pi$ is very large but the low σ value of the membrane renders $\sigma\Delta\Pi$ low. Alternately, if the the concentration in which the membrane is imbibed is dilute, then $\sigma\Delta\Pi$ is very low because $\Delta\Pi$ is very low.

ACKNOWLEDGMENTS

The authors wish to thank Dr. Richard M. Wallace for his valuable comments on membrane system behavior. Also helpful were discussions with Drs. Hal Olsen and Yousif Kharaka of the U.S.G.S. Mr. George Richardson aided in the design of the experimental system. The information contained in this article was developed during the course of work under contract DE-AC09-76SR00001 with the U.S. Department of Energy.

REFERENCES

Bredehoeft, J.D., Blyth, C.R., White, W.A. and Maxey, G.B. (1963) Possible mechanisms for concentration of brines in subsurface formations. Am. Assoc. Pet. Geol. Bull., 47, 257-269.

Caplan, S.R. and Mikulecky, D.C. (1966) Transport processes in membranes. in: Ion Exchange, I: J.A. Marinsky, ed., Marcel Dekker, N.Y., 45-79.

Coplen, T.B. and Hanshaw, B.B. (1973) Ultrafiltration by a compacted clay membrane, I. Oxygen and hydrogen isotopic fractionation. Geochim. Cosmochim. Acta, 37, 2295-2310.

Dainty, J. and Ginzburg, B.G. (1964) The measurement of hydraulic conductivity of internodal characean cells by means of transcellular osmosis. Biochim. Biophys. Acta, 102-111.

Elrick, D.E., Smiles, D.E., Baumgartner, N., and Groenevelt, P.H. (1976) Coupling phenomena in saturated homo-ionic montmorillonite: I. Experimental. Jour. Soil Sci. Soc. Amer. 40, .

Glasstone, S. (1946) Textbook of physical chemistry. Van Nostrand, New York.

Goldstein, D.G. and Solomon, A.K. (1960) Determination of equivalent pore radius for human red cells by osmotic pressure measurement. J. Gen. Physiol. 44, 1-17.

Hanshaw, B.B. (1962) Membrane properties of compacted clays, Ph.D. dissertation, Harvard Univ., Cambridge Mass. 113 p.

Hanshaw, B.B. (1963) Cation exchange constants for clays from electrochemical measurements. In: Proc. Clays and Clay Mins., 12 th Nat. Conf., 397-421.

Hanshaw, B.B. (1972) Natural-membrane phenomena and subsurface waste emplacement. In: Underground Waste Management and Environmental Implications. Am. Assoc. Petr. Geol. Memoir 18., Tulsa. 308-315.

Hanshaw, B.B. and Hill, G.(1969) Geochemistry and hydrodynamics of the Paradox Basin region, Utah, Colorado and New Mexico. Chem. Geol. 4, 263-294.

Hanshaw, B.B. and Zen, E. (1965) Osmotic equilibrium and overthrust faulting. Geol. Soc. Am. Bull. 76, 1379-1387.

Harned, H.S. and Owen, B.B. (1958) The Physical Chemistry of Solutions. Reinhold, New York.

Katchalsky, A. and Curran, P.F. (1965) Non-Equilibrium Thermodynamics in Biophysics. Harvard University Press, Cambridge. 248 p.

Kedem, O., and Katchalsky, A. (1963) Permeability of composite membranes. I: Electric current, volume flows and flow of solute through membranes. Trans. Faraday Soc. 59, 1918-1930

Kemper, W.D., and Rollins, J.B. (1966) Osmotic efficiency coefficients across compacted clays. Soil Sci. Soc. Am. Proc 30, 529-534.

Kharaka, Y.K., and Berry, F.A. (1973) Simultaneous flow of water and solutes through geologic membranes, I. Experimental investigation. Geochim. Cosmochim Acta 37, 2577-2603.

Marine, I.W. and Fritz, S.J. (1981)Osmotic model to explain anomalous hydraulic heads. Water Resources Res. 17, 73-82.

McKelvey, J.G. and Milne, I.H. (1962)The flow of salt solutions through compacted clay. Clays and Clay Min. 9, 248-259.

Miller, D.G. (1966) Applications of irreversible thermodynamics to electrolyte solutions. I. Determination of ionic transport coefficients l_{ij} for isothermal vector transport processes in binary electrolyte systems. J. Phys. Chem. 70, 2639-2659.

Olsen, H.W. (1969) Simultaneous fluxes of liquid and charge in saturated kaolinite. Soil Sci. Soc. Am. Proc. 33, 338-344.

Porter, M.C. (1979)Membrane filtration. In Handbook of Separation Techniques for Chemical Engineers, P.A. Schweitzer, ed., McGraw-Hill New York.

Sriyastava, R.C. and Avasthi, P.K. (1975) Non-equilibrium thermodynamics of thermo-osmosis of water through kaolinite. J. Hydrology 24, 111-120.

Staverman, A.J. (1952) Non-equilibrium thermodynamics of membrane processes. Trans. Faraday Soc. 48, 176-185.

Young, A. and Low, P.F. (1965) Osmosis in argillaceous rocks. Am. Assoc. Pet. Geol. Bull.49 (), 1004-1008.

Run	Porosity in Percent	Steady State Solution Flux (J_v) x 10^{-6} $cm \cdot sec^{-1}$	NaCl Molarity in Syringe Pump (C_i)	Steady State NaCl Molarity in Effluent (C_e)	$\bar{C}_x$ in moles NaCl per cm^2 of frit	K as calculated by equation 20	C_o in NaCl Molarity from $C_o = \frac{C_e}{K}$	$\sigma = \frac{C_o - Ce}{C_o + C_e}$	Theoretical $\Delta\pi$ in MPa from $\Delta\pi = 2RT(C_o - Ce)$	Osmotic Back Pressure $\Delta P = \sigma\Delta\pi$ in MPa
1	59	3.33	0.0103	0.0103	0.0339	0.0689	0.1502	0.87	0.69	0.60
2	59	3.15	0.0947	0.0925	0.1619	0.2404	0.3850	0.61	1.44	0.88
3	59	4.96	0.9504	0.9399	1.2238	0.9189	1.0229	0.04	0.41	0.01
4	41	2.79	0.0117	0.0117	0.0397	0.0571	0.2051	0.89	0.95	0.85
5	41	2.31	0.0983	0.0974	0.2054	0.1165	0.8359	0.79	3.65	2.89
6	41	2.92	0.9389	0.9369	1.3009	0.5354	1.7500	0.30	4.02	1.21

Table 1. Hyperfiltration data of the six experimental runs. Experimentally determined values of C_e and J_v at steady state allow calculation of K via equation 20. To use this equation, the amount of NaCl stored in the top frit at steady state must also be known. The $\bar{C}_x$ term is the total number of moles of NaCl in the 48.6 cm^3 porous volume of the frit, multiplied by the CPL thickness of 1.27 cm., equivalent to the thickness of the porous frit.

Run	Volume Fraction of water in Membrane ϕ_w	χ in equivalents per gram	$C_s = \frac{C_i+C_e}{2000}$ C_s in moles NaCl per cm^3	$\bar{C}_a$ in moles NaCl per cm^3 of membrane	$\bar{C}_a/\bar{C}_c = \frac{\bar{C}_a}{\bar{C}_a+\chi}$	Distribution Coefficient of Salt in Membrane $K_s = \frac{\bar{C}_a}{C_s}$	"Best Fit" R_{wm}	σ calculated from equation 25	σ calculated from experimental data (equation 24)
1	0.59	9.84×10^{-4}	8.0×10^{-5}	2.3×10^{-6}	2.31×10^{-3}	0.0283	0	0.87	0.87
2	0.59	9.84×10^{-4}	2.39×10^{-4}	1.98×10^{-5}	1.97×10^{-3}	0.0828	0	0.64	0.61
3	0.59	9.84×10^{-4}	9.81×10^{-4}	2.678×10^{-4}	2.139×10^{-1}	0.2729	0	0.09	0.04
4	0.41	1.416×10^{-3}	1.08×10^{-4}	1.4×10^{-6}	9.8×10^{-4}	0.0128	0.10	0.92	0.89
5	0.41	1.416×10^{-3}	4.67×10^{-4}	2.54×10^{-5}	2.111×10^{-2}	0.0544	0.10	0.69	0.79
6	0.41	1.416×10^{-3}	1.343×10^{-3}	1.890×10^{-4}	1.1777×10^{-1}	0.1407	0.10	0.31	0.30

Table 2. A comparison of σ values obtained by experiment with that calculated from the Fritz-Marine Membrane Model. The measured parameters needed to calculate σ via equation 25 are listed. In this equation, the values of R_w and R_m are assumed to be 1.63 and 1.8, respectively. For runs at a given porosity, the value of R_{wm} was used to obtain the closest fit between σ calculated from equation 25 versus that obtained from the hyperfiltration data.

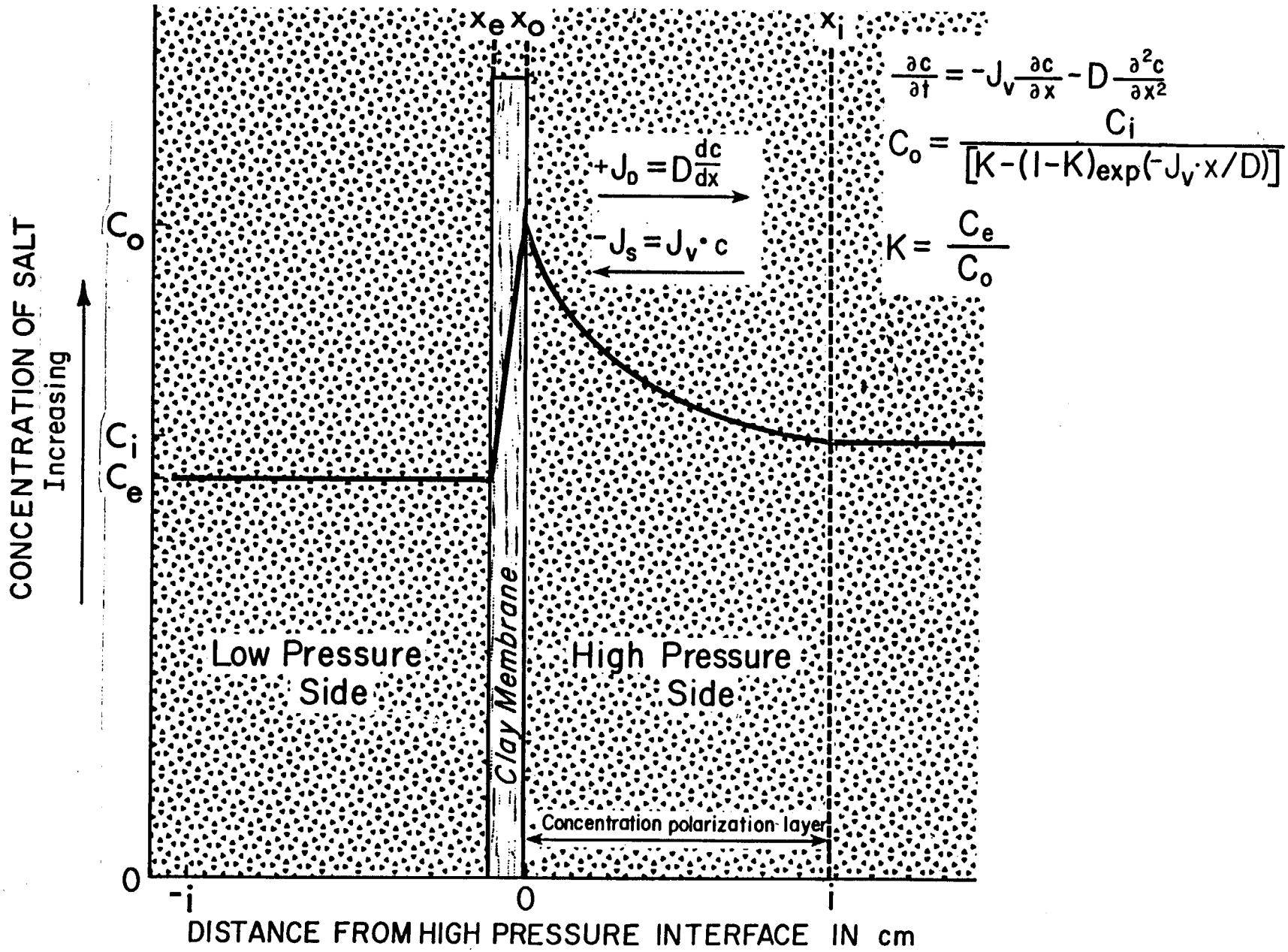

Figure 1. A Schematic diagram of hyperfiltration through a clay membrane positioned between two sandstone units. Initially solute concentration within the pores of both sandstone units is equal to C_i. With the onset of hyperfiltration, solute steady state, $\partial C/\partial t$ is zero and the build-up of solute at the high pressure interface defines the concentration polarization layer, CPL.

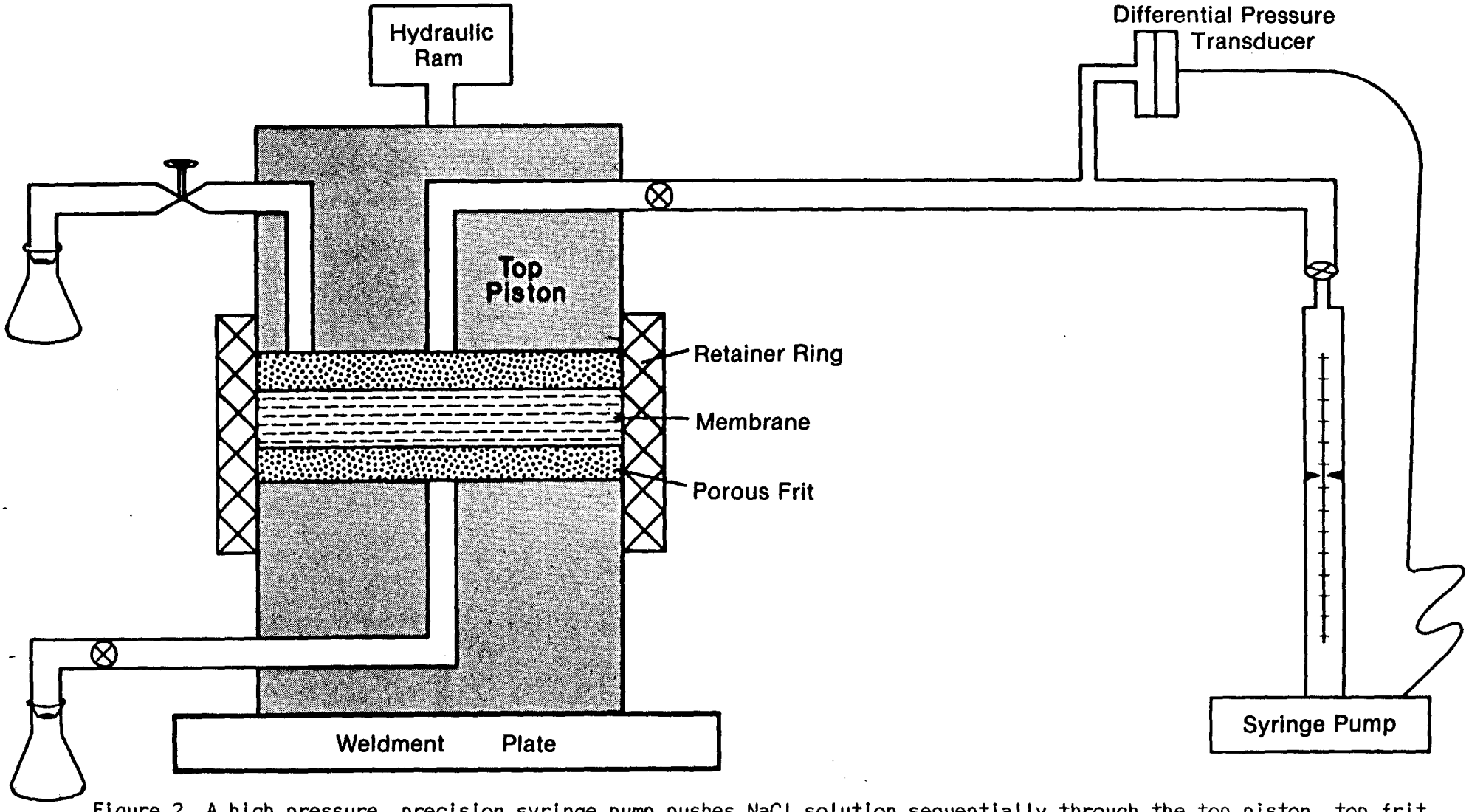

Figure 2. A high pressure, precision syringe pump pushes NaCl solution sequentially through the top piston, top frit, clay membrane, and the bottom frit. The solution exiting the bottom piston is collected in a pre-weighed Erlenmeyer flask. Periodically, the needle valve on the high pressure (top piston) side of the membrane is opened to allow collection of the solution which is bypassed at the frit/top-piston interface. This procedure insures no build-up of solute concentration at this interface by the concentration polarization effect. A differential pressure transducer is valved into the line to maintain a hydraulic pressure gradient across the membrane at a constant 17.5 MPa.